Miniaturization of an optoelectronic holographic otoscope for measurement of nanodisplacements in tympanic membranes

Geoffrey Karasic – Nathan Largesse – Lucas Samuel Lincoln
Advisor: Cosme Furlong
Mechanical Engineering Department
CHSLT – ME
Center for Holographic Studies and Laser µmechaTronics

Objective

To improve, miniaturize, and validate the optical head of a previously developed Opto-Electronic Holographic Otoscope (OEHO).

Methods

- Investigated relevant biology to identify potential areas of improvement of the optical head
- Designed and analyzed an optical configuration using ray tracing optical design software
- Manufactured prototype optical head, and analyzed optical characteristics
- Followed ACES methodology, which compares analytical, computational, and experimental solutions to validate the developed optical head

Introduction

The Opto-Electronic Holographic Otoscope is an otology tool developed at the CHSLT for the Massachusetts Ear and Eye Infirmary (MEEI) which allows for full-field, video rate, nanometer-scale deformation of mammalian tympanic membranes (TM). The first generation system is currently being used in a laboratory environment at MEEI to gather quantitative data about normal and pathological TM to better understand human hearing and hearing disorders.

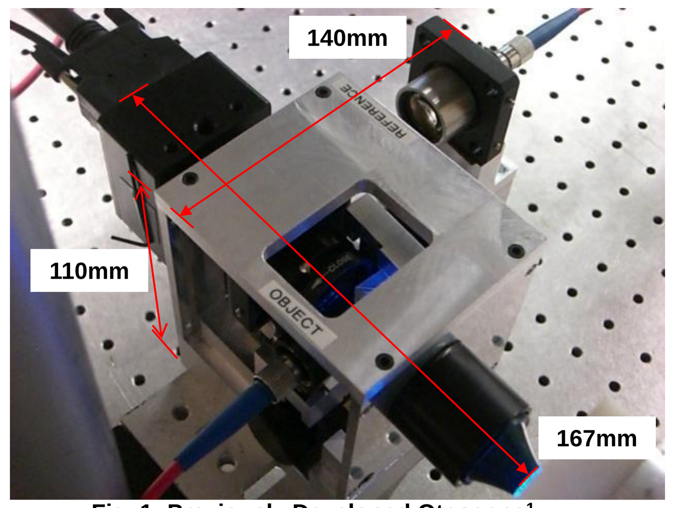

Fig. 1: Previously Developed Otoscope[1]

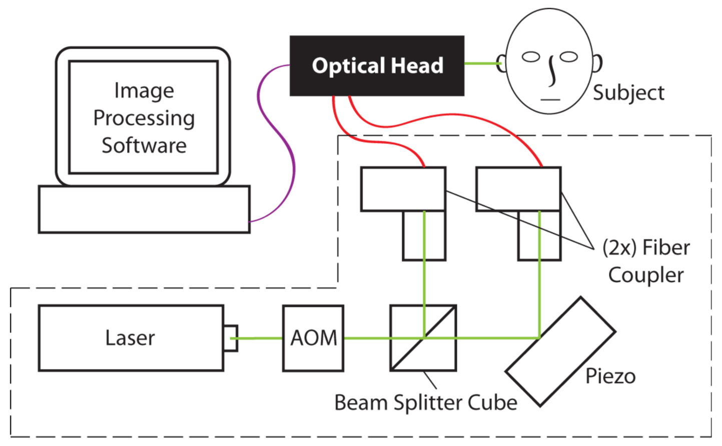

Fig. 2: Laser Delivery System

Based on the devices current in use, several areas of improvement have been identified which much be addressed before the device is deployed for clinical use.

Proposed Improvements:

- Increased thermomechanical stability
- Miniaturization
- Shorter working distance
- Easier and more intuitive focusing and magnification selection
- Increased ergonomics

The goal of this MQP was to address these improvements by redesigning the optical head component of the otoscope system.

Histology, Function, and Optical Properties of TM

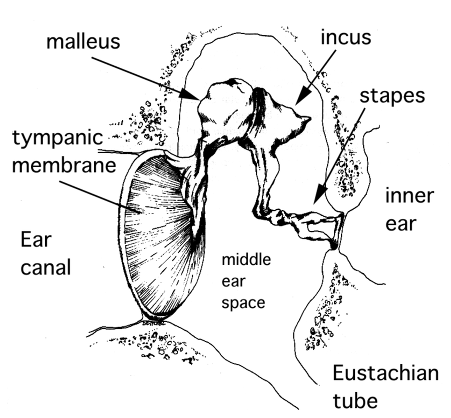

Fig. 3: Anatomy of Middle Ear[2]

- Sound, a vibration in the air, travels down the auditory canal and strikes the tympanic membrane directly.
- The sound energy causes the TM to vibrate precisely accordingly.
- From the footplate of the stapes, the sound energy travels through a fluid in the inner ear.

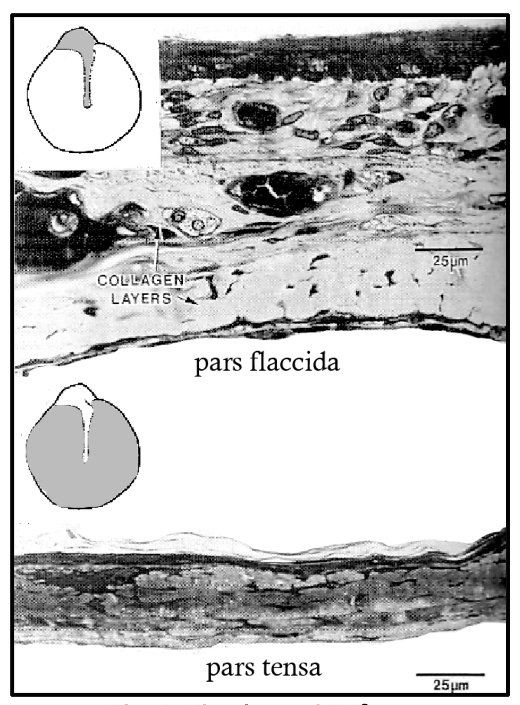

Fig. 4: Histology of TM[3]

- It has two components: the pars flaccida and the pars tensa of thickness 110µm and 34µm, respectively

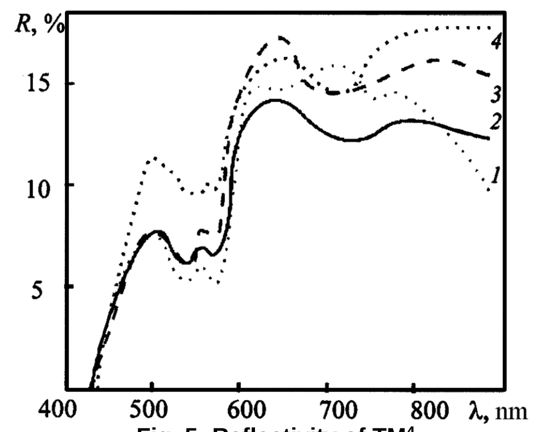

Fig. 5: Reflectivity of TM[4]

- The TM is difficult to study optically due to its in-homogeneity, multiple layers, and the anisotropy of their physical characteristics.
- TM reflects the most light (~13%) at wavelengths between 630 and 1000 nm.
- White Chinese ink and magnesium oxide applied to the surface of TM can improve mean reflected intensity by 40%

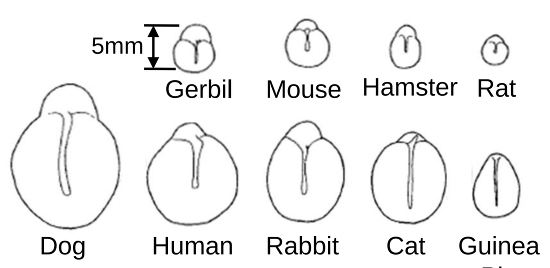

Fig. 6: Relative Sizes and Shapes of Mammalian TMs[3]

- The human TM is elliptical in shape, measuring horizontally 9-10mm and vertically 8-9mm

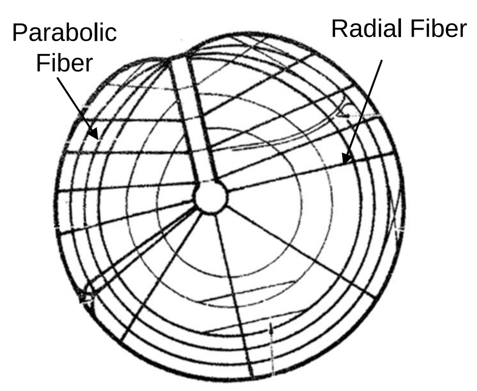

Fig. 7: Fiber Array in Human TM showing Radial and Parabolic Fibers[5]

- The mechanical properties of the TM are determined by complex fiber array found in the lamina propia layer of the TM

Design Requirements

- Depth of field must be approximately 5mm
- Field of view must be on the order of 10mm in diameter
- Should be capable of measuring at frequencies between 16Hz and 20kHz
- Must have a measuring resolution on the order of several nanometers

Otoscope Design

Design of the optical head was supported by CAD software featuring ray tracing analysis of light propagation[6].

The software performs ray transfer matrix analysis. An optical component, or system of components, is represented by a **ray transfer matrix** (RTM)[7].

$$\begin{bmatrix} r' \\ \theta' \end{bmatrix} = \begin{bmatrix} A & B \\ C & D \end{bmatrix} \begin{bmatrix} r \\ \theta \end{bmatrix}$$

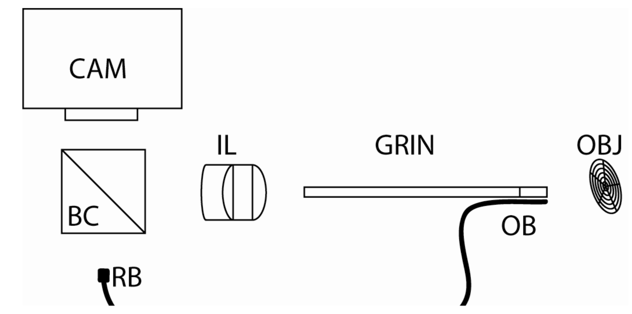

Fig. 8: Otoscope Head Schematic

The derivation of the RTM for the GRIN material requires discretization of thin material slices, as the refractive index varies in the material according to[7]:

$$n(r) := n_0 \cdot \left(1 - \frac{\alpha^2}{2} r^2\right)$$

$$T(\delta z) := \begin{pmatrix} 1 & \frac{\delta z}{n_0} \\ 0 & 1 \end{pmatrix} \qquad R(\delta z) := \begin{bmatrix} 1 & 0 \\ (n_0 \cdot \alpha)^2 \delta z & 1 \end{bmatrix}$$

$$M(\delta z) = T(\delta z) \cdot R(\delta z) = \begin{bmatrix} 1 - (\alpha \cdot \delta z)^2 & \frac{\delta z}{n_0} \\ -n_0 \cdot \alpha^2 \cdot \delta z & 1 \end{bmatrix}$$

$$\text{Substitute } K := \alpha \cdot n_0 \qquad \alpha \cdot \delta z = 2 \cdot \sin\left(\frac{\theta}{2}\right)$$

$$M(\delta z) := \begin{pmatrix} 2\cos(\theta) - 1 & \frac{2 \cdot \sin\left(\frac{\theta}{2}\right)}{K} \\ -2 \cdot K \cdot \sin\left(\frac{\theta}{2}\right) & 1 \end{pmatrix}$$

$$M(t) = \begin{pmatrix} \cos(p \cdot \theta) & \frac{\sin(p \cdot \theta)}{K} \\ -K \cdot \sin(p \cdot \theta) & \cos(p \cdot \theta) \end{pmatrix} = \begin{pmatrix} \cos(\alpha \cdot t) & \frac{\sin(\alpha \cdot t)}{n_0 \cdot \alpha} \\ -n_0 \cdot \alpha \cdot \sin(\alpha \cdot t) & \cos(\alpha \cdot t) \end{pmatrix}$$

n = refractive index
n_o = refractive index on axis
α = index coefficient, equal to reciprocal of radius at which $n = n_0 / 2$
T(δz) = translation matrix for slice of thickness δz
R(δz) = refraction matrix for slice of thickness δz
p = number of discrete steps used to represent 't' length GRIN material
t = p · δz, length of GRIN material

Likewise, the imaging achromat RTM was computed:

$$\begin{pmatrix} A & B \\ C & D \end{pmatrix} := \begin{pmatrix} 0.918 & 2.774 \times 10^{-3} \\ -100.114 & 0.787 \end{pmatrix}$$

IL Focal points:

$$\frac{D}{C} = -7.861 \times 10^{-3} \cdot m$$

$$\frac{-1}{C} = 9.989 \times 10^{-3} \cdot m$$

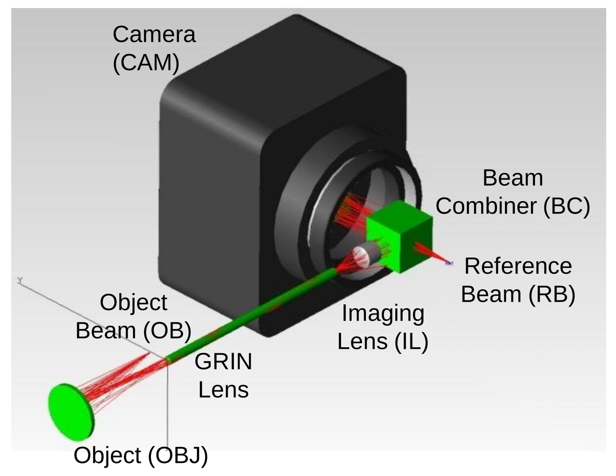

Fig. 9: Ray Tracing Schematic

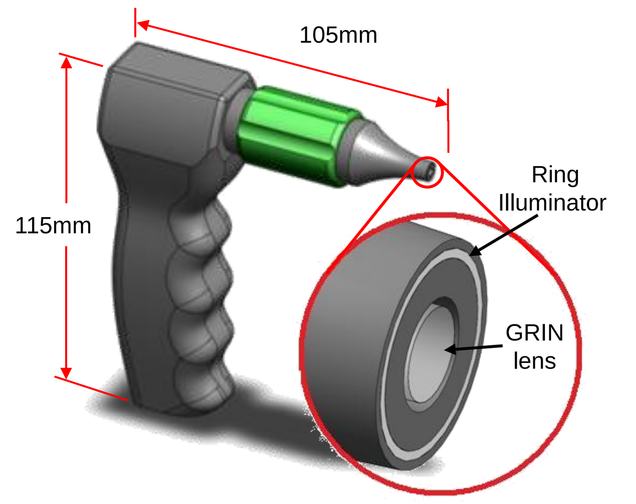

Fig. 10: Rendering of Packaged Optics

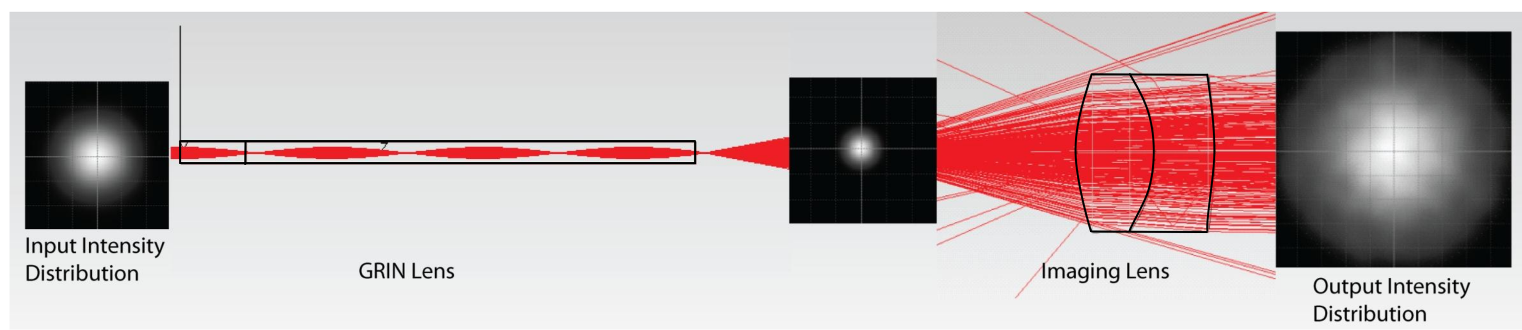

Fig. 11: Computational Analysis of Light Propagation Through Optical System Showing Effects of Optical Components on the Quality of the Transmitted Waveform Distributions

Realization

The head was constructed and characterized to quantitatively measure its optical performance.

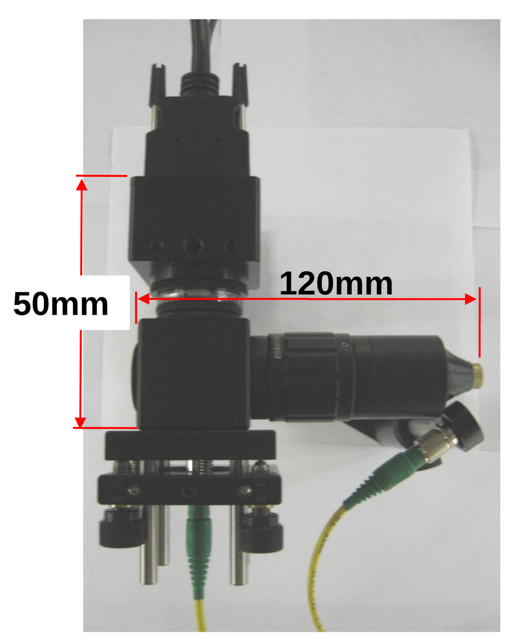

Fig. 12: Otoscope Dimensions

Depth of Field

- 6.2mm
- Able to resolve 5 line pairs per millimeter at 60% contrast from 9.9mm to 16.1mm when focused at the working distance of 13mm


Fig. 13: Depth of Field Test

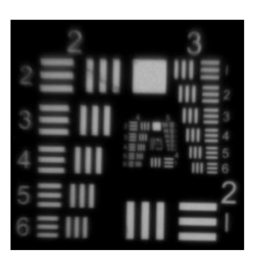
Fig. 14: USAF Resolution Target

Resolution

- 11.30 line pairs per millimeter were resolved with 59% contrast (Group 3 Element 4)

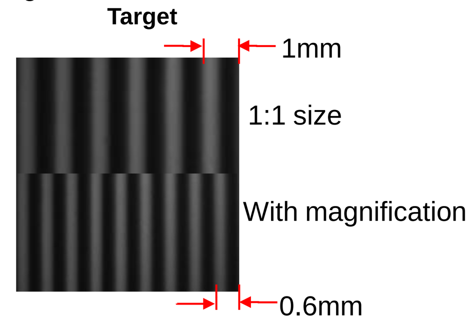

Fig. 15: Magnification Target

Field of View & Magnification

- 10mm x 10mm field of view at a 13mm working distance
- 0.6 a 13mm working distance

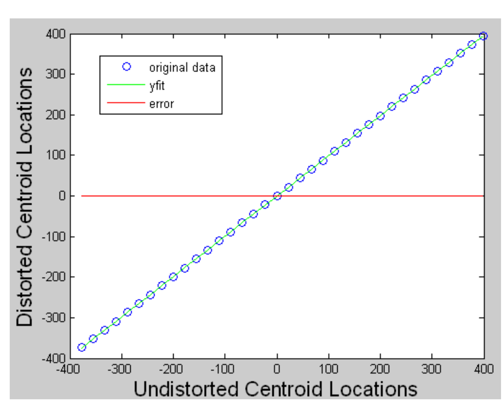

Fig. 16: Distortion Function Curve Fit

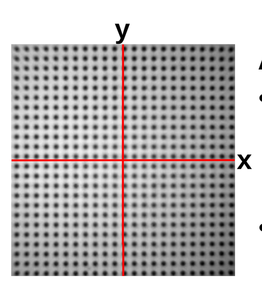

Fig. 17: Grid Target

Aberration

- Distortion function: how the image along the abscissa, x, and ordinate, y, in Cartesian coordinates is distorted
- Determined equation describing optical aberration:

$$y'(y) = -4.038 \cdot 10^{-8} \cdot y^3 + -3.729 \cdot 10^{-6} \cdot y^2 + 0.995 \cdot y + -0.327$$

Validation

The frequency for the first three modes of vibration of a cantilever beam were determined analytically, experimentally, and computationally.

Copper Beam[8] Dimensions: 10.69mm × 4.47mm × 0.51mm

	First Mode	Second Mode	Third Mode
Analytical	244.3 Hz	1531.3 Hz	4287.6 Hz
Experimental Data was acquired using otoscope head in double exposure mode with stroboscopic illumination.	238.5 Hz 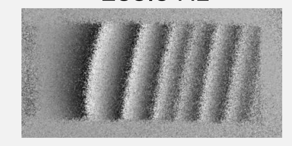	1501.5 Hz 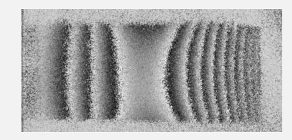	4092.0 Hz 
Finite Element Method	244.9 Hz 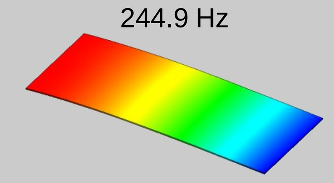	1534.7 Hz 	4297.1 Hz 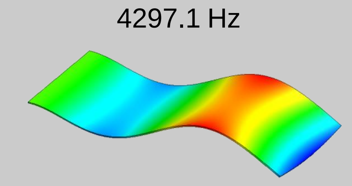

Percent Error with Respect to Experimental Values

	First Mode	Second Mode	Third Mode
Analytical	2.4 %	2.0 %	4.9 %
Computational	2.7 %	2.2 %	5.0 %

- The minimal error (<5%) between the analytical and computational frequencies compared with the experimentally determined frequencies validates the otoscope head.
- The system was also validated by measuring dynamic deflections of a thin nitrile membrane.

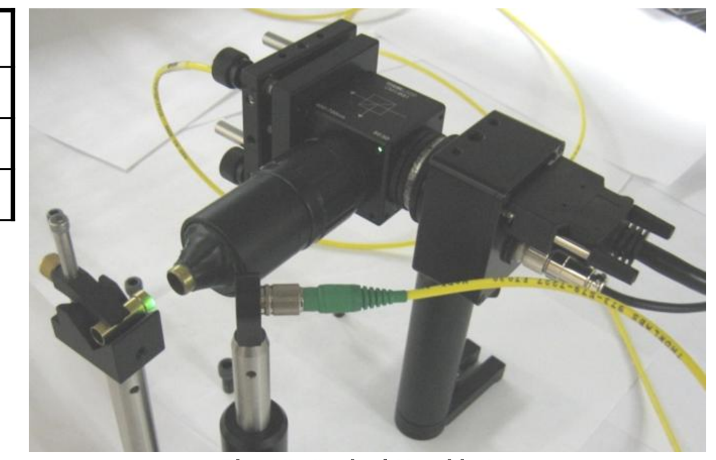
Fig. 18: Optical Head in Use

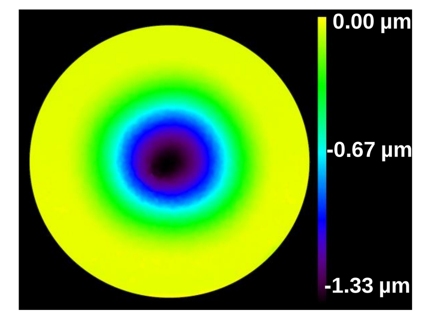

Fig. 19: Deflection of Nitrile Membrane at 4.228kHz

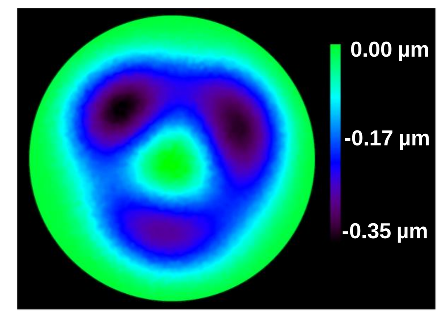

Fig. 20: Deflection of Nitrile Membrane at 10.66kHz

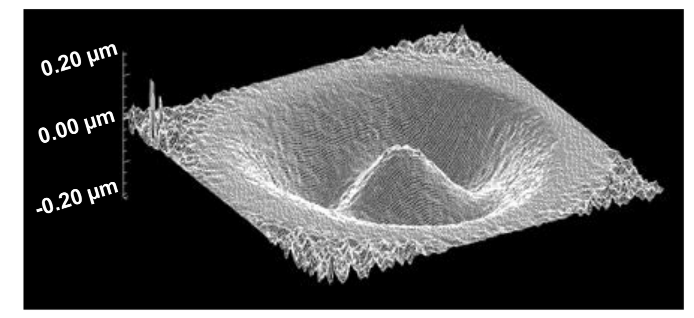

Fig. 21: 3D Representation of Nitrile Membrane at 10.66kHz

Experiments on Chinchilla Tympanic Membrane

Medical professionals from the Massachusetts Eye and Ear Infirmary experimented with the updated otoscope head, taking measurements of a cadaveric chinchilla membrane as seen in Figs 22 to 24.

Fig. 22: Postmortem Chinchilla Specimen

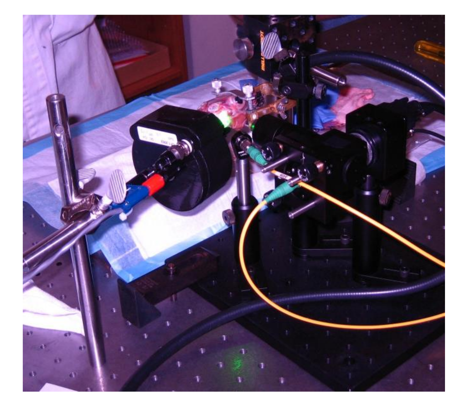
Fig. 23: Chinchilla TM Testing

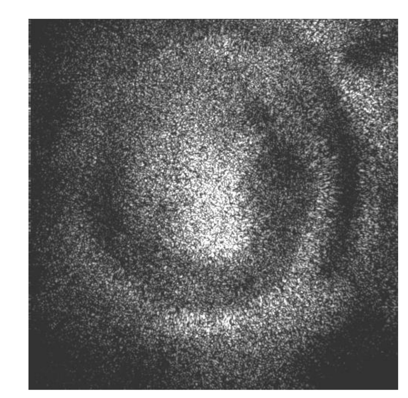
Fig. 24: Time Average Interferogram of Chinchilla TM

Conclusions and Future Works

The optical head has been quantitatively characterized for direct comparisons against future generations. Tests performed at the CHSLT shown improved characteristics in many of the desired areas, including depth of field; increased ease of use (including focusing and magnification) for the physician; and a more miniaturized package that resembles existing otoscopes. The device was validated via comparison of analytical, computational, and experimental solutions.

To further improve the utility of this device it is recommended that:

- Thermomechanical stability continues to be improved. Investigations into the feasibility of single-fiber-to-head system should be paramount.
- An illumination system, which provides even object beam illumination inside the ear canal, is incorporated into the optical head. Fiber optic bundles and ring-illumination should be investigated as potential solutions.
- More common, near-infrared lasers should be used as they will provide a better response from the TM and have better optical component support.
- PCB board versions of the existing camera are available and will provide greater packaging options and size savings.

References

[1] Dywer, B., Maccaferri, M., Wester, C., "Design and Realization of a Laser Holographic Otoscope," *MQP, WPI-ME*, 2008
[2] Phon.ox.ac.uk. Home Page. Retrieved 15 December 2008, http://www.phon.ox.ac.uk/~jcoleman/speaking_hearing.htm
[3] Chole, R.A., Kodama, K., "Comparative histology of the tympanic membrane and its relationship to cholesteatoma," *Ann. Otol. Rhinol. Laryngol.,* 98:761-766, 1989
[4] Doladov, M.Yu., Kazakevich, V.S., Kalashnikov, I.G., Kupaeva, V.V., Shcherbakov, V.A., "Optical reflection of the human tympanic membrane," *J. App.Spectroscopy,* 66:708-710, 2001
[5] Lim, D.J., "Structure and function of the tympanic membrane: a review," *Acta oto-rhino-laryngologica Belg.,* 49:101-115, 1995
[6] TracePro a Lambda Research Product. Licensed to WPI/CHSLT, 2008
[7] Gerrard, A., *Introduction to Matrix Methods in Optics,* John Wiley & Sons, NY, 1975
[8] Oberg, E. et al., *Machinery's Handbook: 28th Edition,* Industrial Press, NY, 2008

ACKNOWLEDGEMENTS: Supported by the NIDCD, WPI, MEEI, and the Mittal Fund.